Molecular Cell, Volume *67*

Supplemental Information

Smarcal1-Mediated Fork Reversal Triggers Mre11-Dependent Degradation of Nascent DNA in the Absence of Brca2 and Stable Rad51 Nucleofilaments

Arun Mouli Kolinjivadi, Vincenzo Sannino, Anna De Antoni, Karina Zadorozhny, Mairi Kilkenny, Hervé Técher, Giorgio Baldi, Rong Shen, Alberto Ciccia, Luca Pellegrini, Lumir Krejci, and Vincenzo Costanzo

Figure S1, related to Figure 1

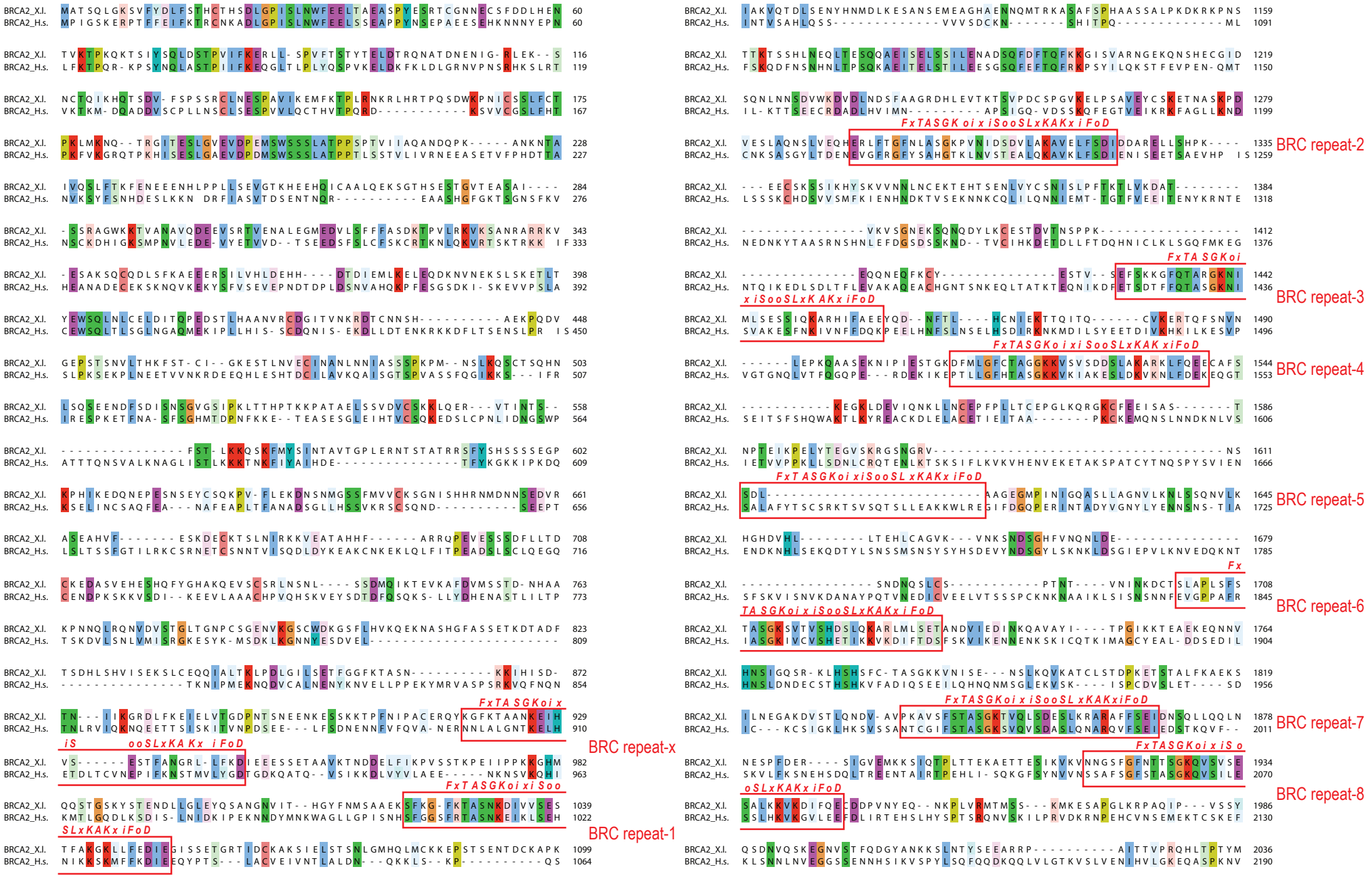

[*TASGKoixiSooSLxKAKxi FoD*] = BRC repeat-consensus; o=polar, i=hydrophobic, x=any aa

Figure S2, related to Figure 1

A

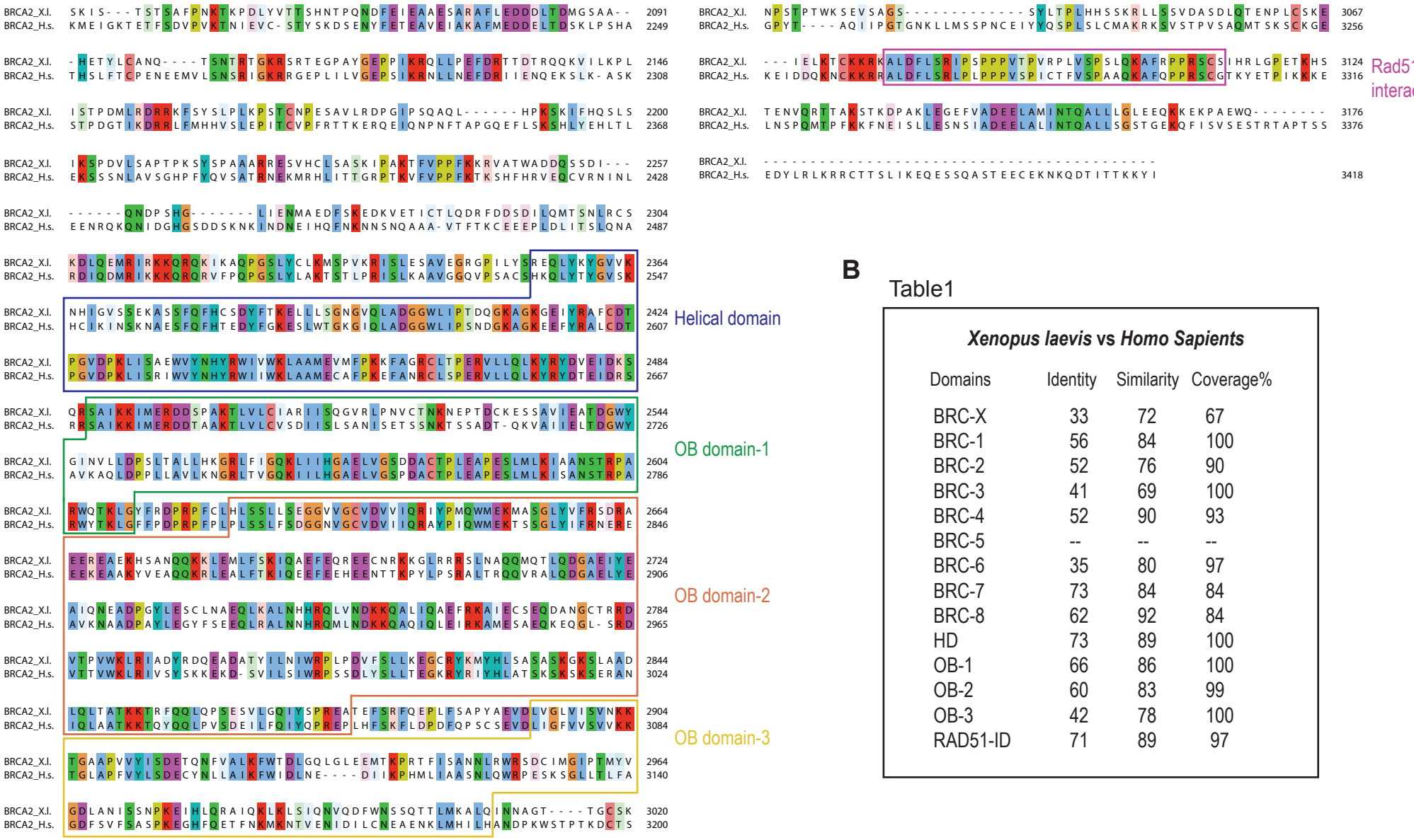

B

Table1

Xenopus laevis* vs *Homo Sapients

Domains	Identity	Similarity	Coverage%
BRC-X	33	72	67
BRC-1	56	84	100
BRC-2	52	76	90
BRC-3	41	69	100
BRC-4	52	90	93
BRC-5	--	--	--
BRC-6	35	80	97
BRC-7	73	84	84
BRC-8	62	92	84
HD	73	89	100
OB-1	66	86	100
OB-2	60	83	99
OB-3	42	78	100
RAD51-ID	71	89	97

Figure S3, related fo Figure 1

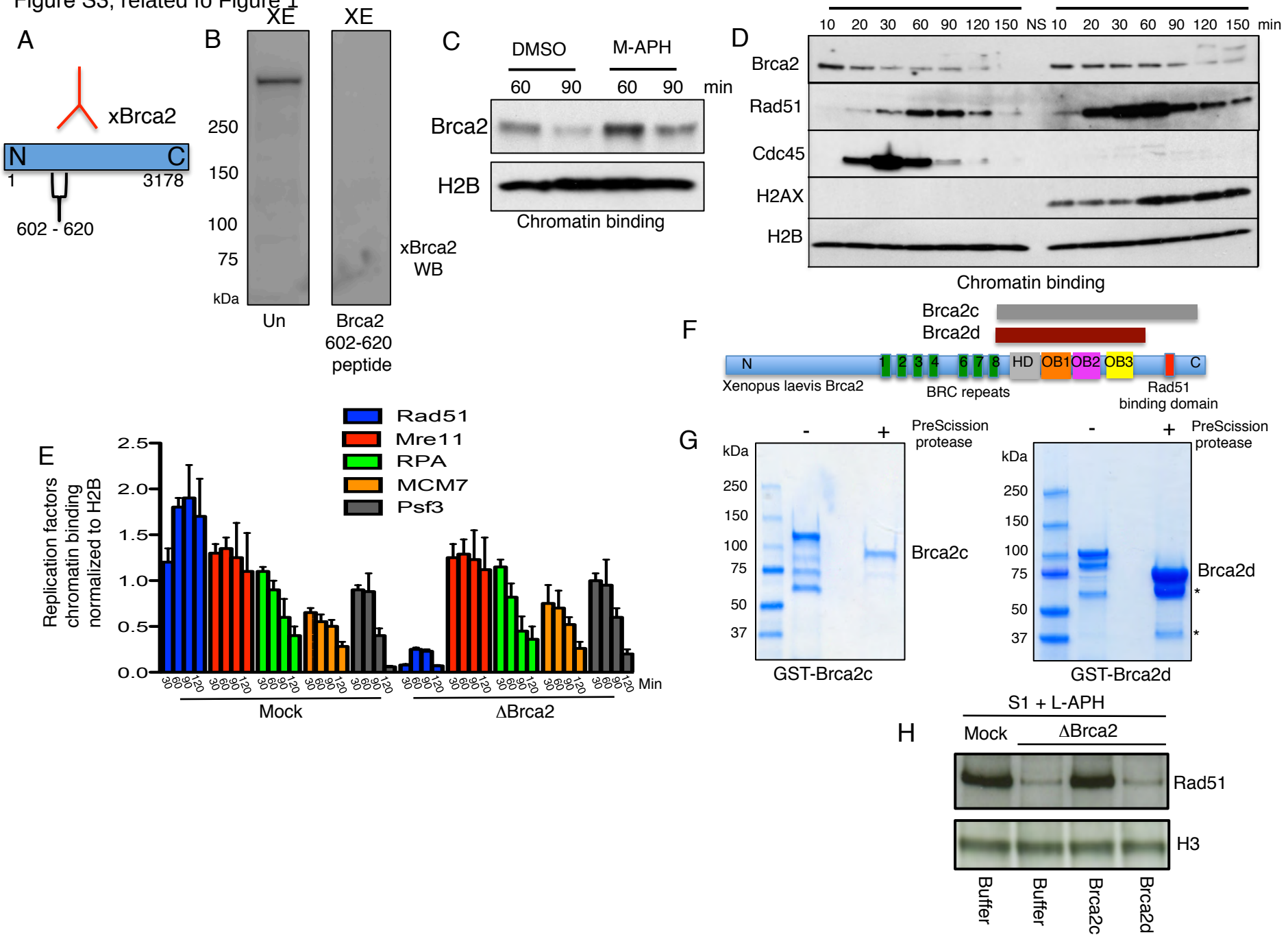

Figure S4, related to Figures 2-3

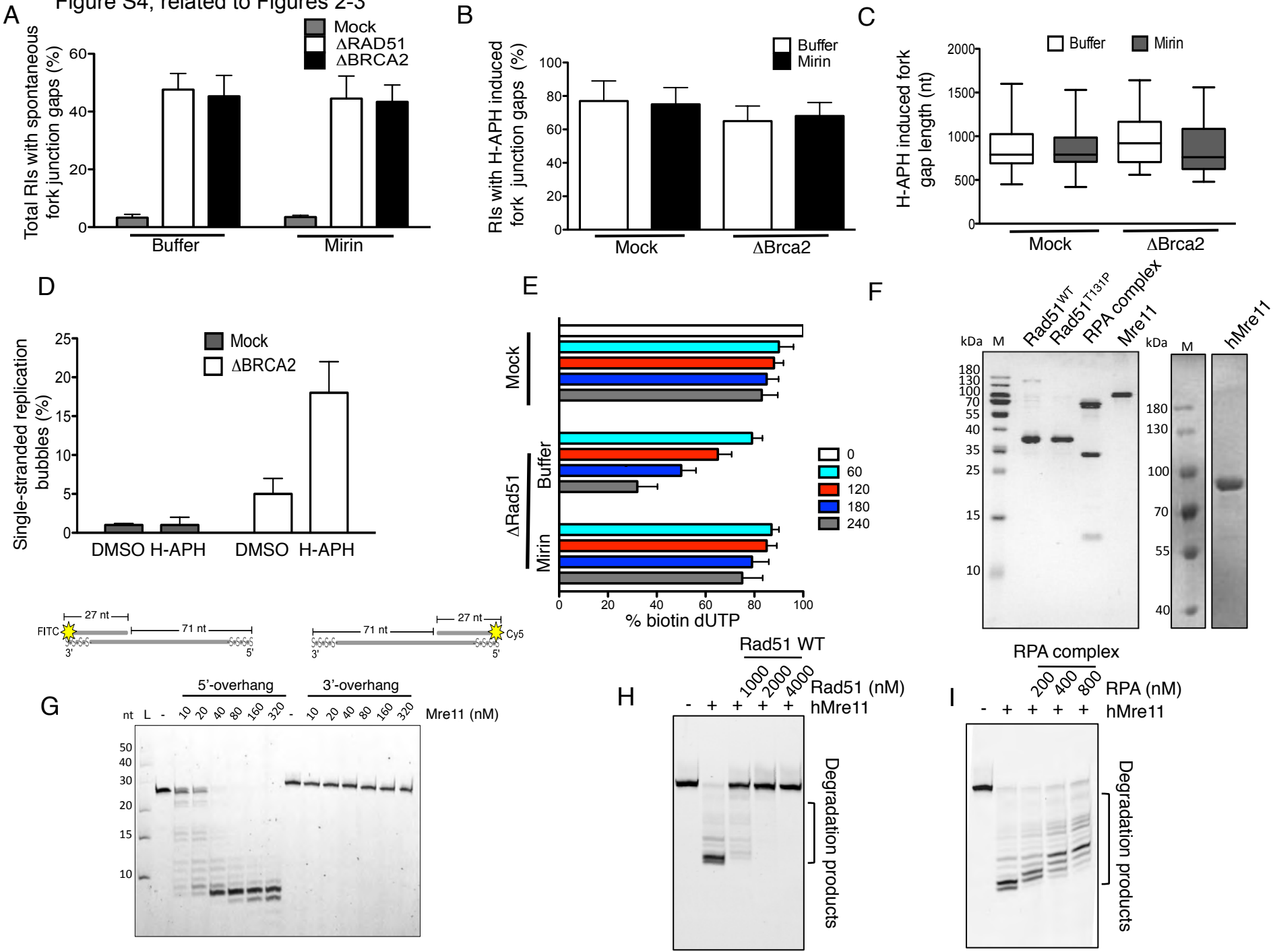

Figure S5, related to Figure 3

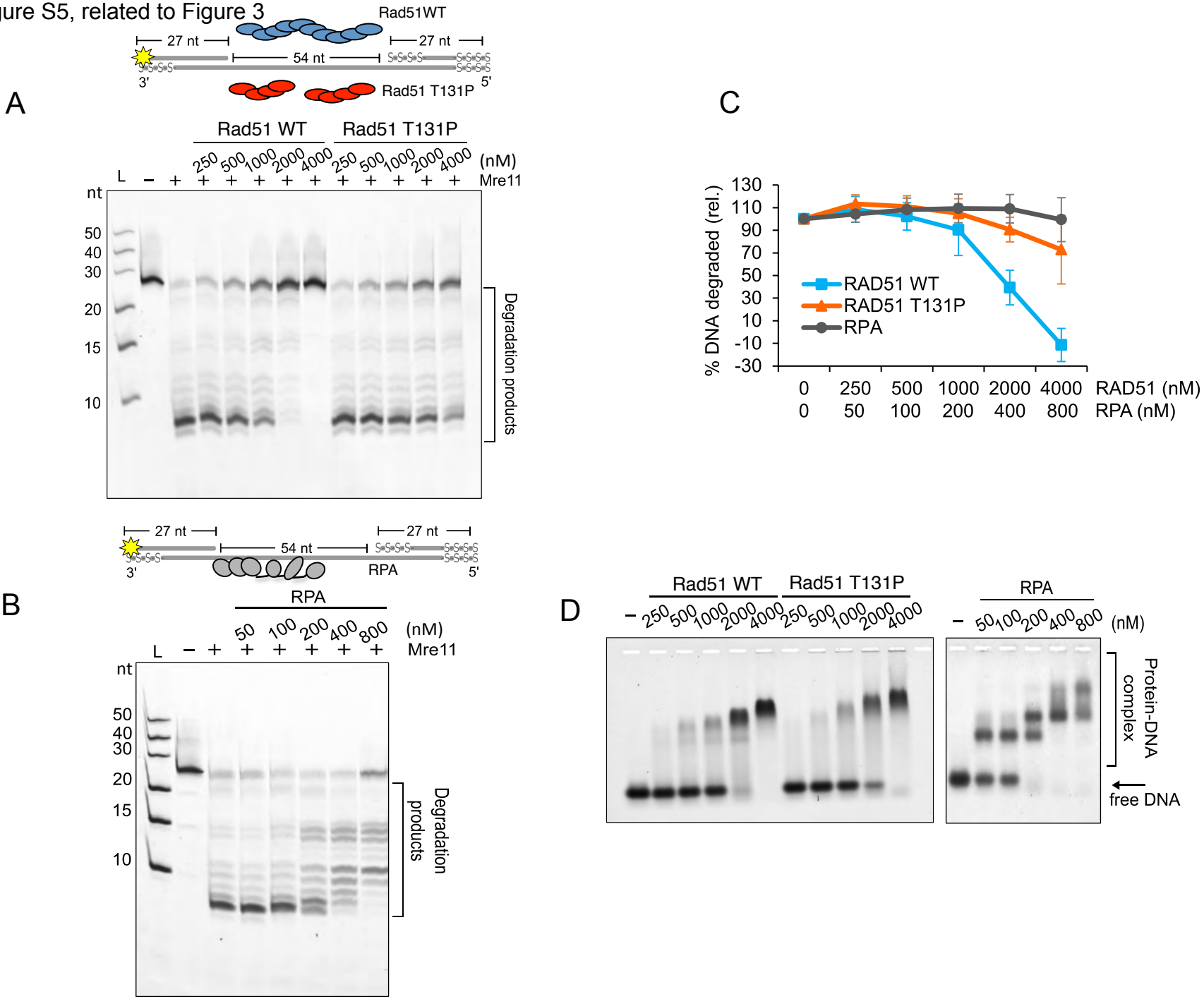

Figure S6, related to Figure 4

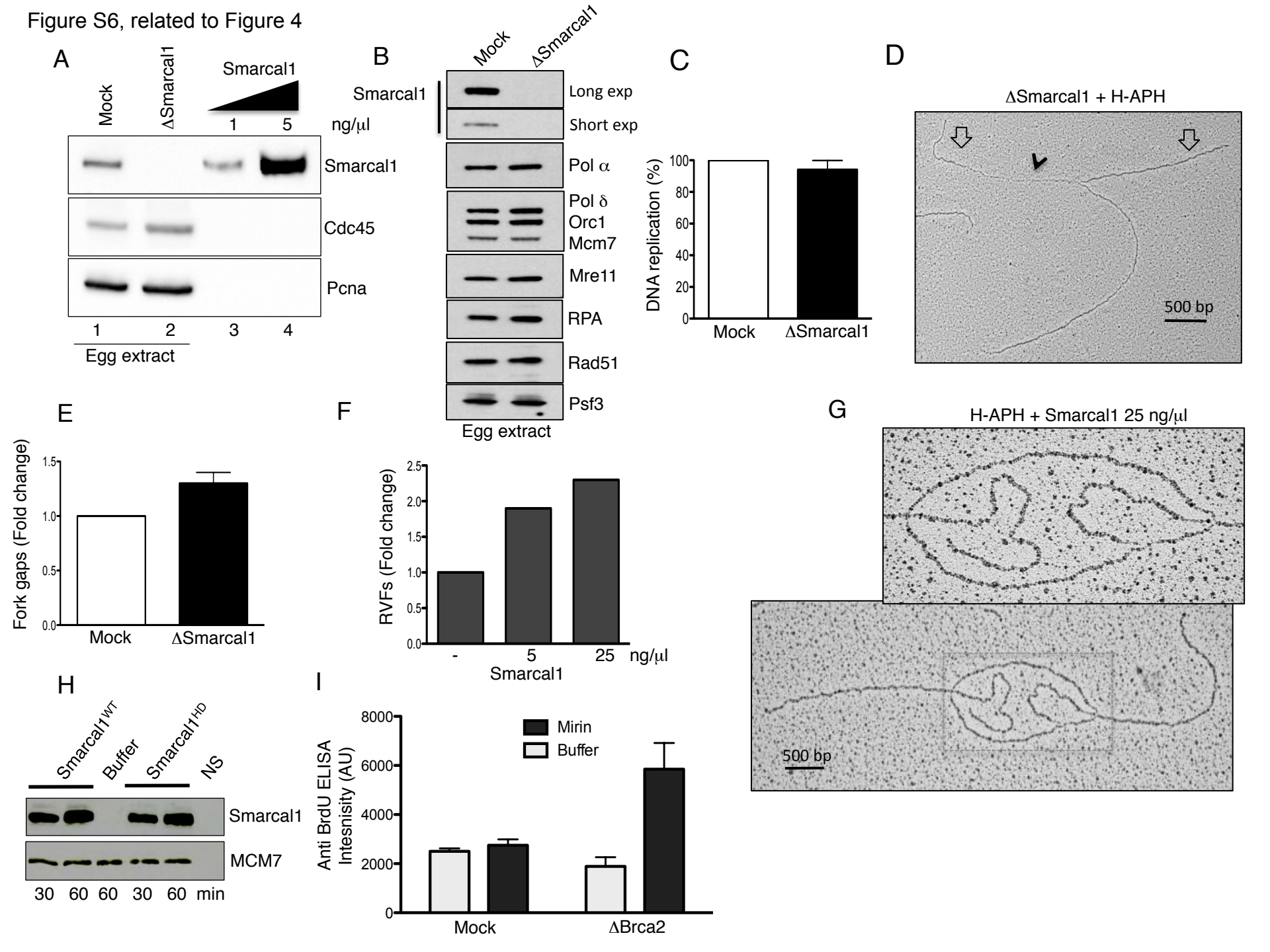

Figure S7, related to Figure 6

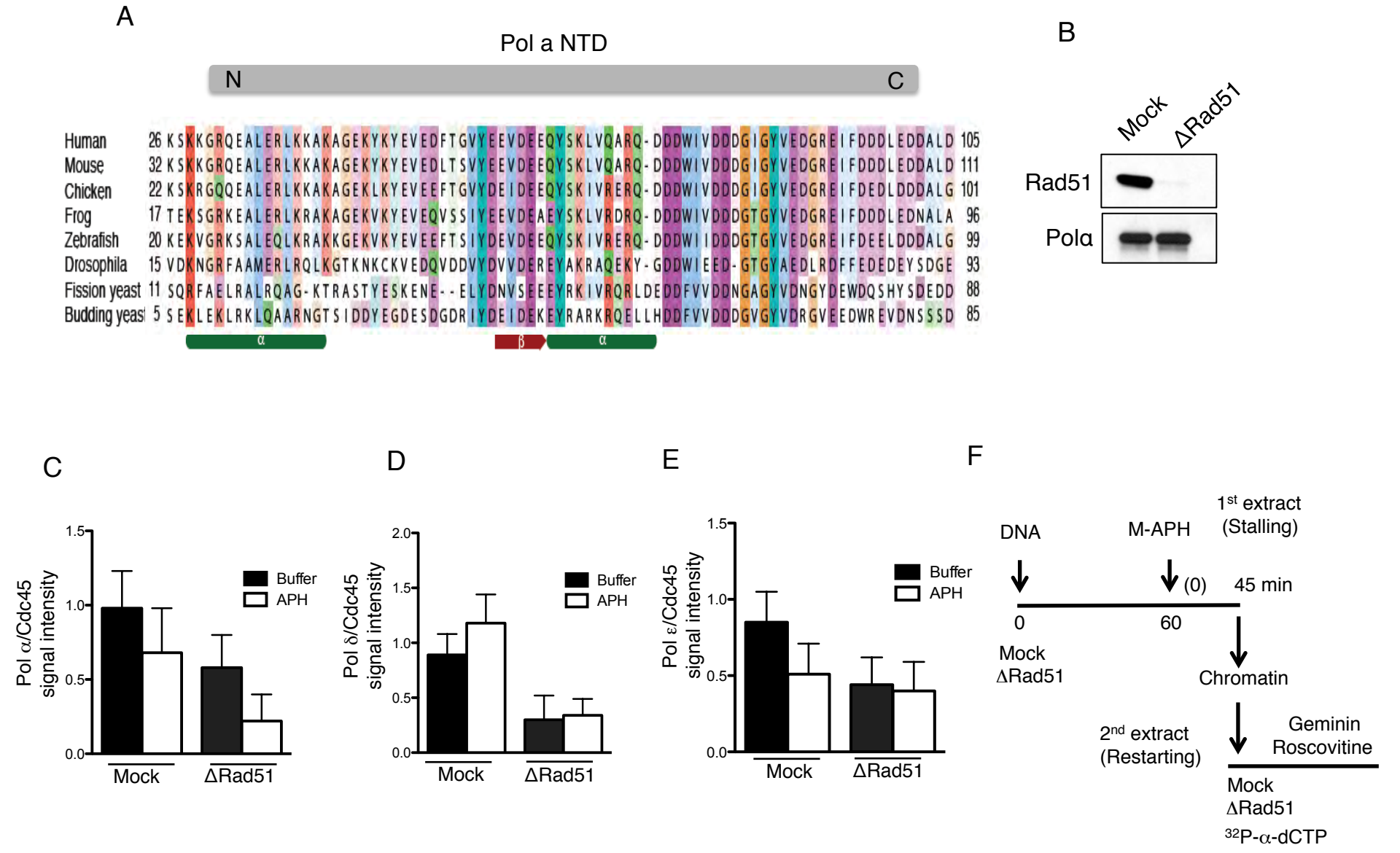

Supplementary Figure Legend

Supplementary Figure S1. *Xenopus* Brca2 protein (N-terminal half). Alignment of *Xenopus* and human Brca2 proteins including the region containing the BRC repeat domains (highlighted) with amino acids colored according to conservation and chemical nature. Protein sequences alignment was done using Clustal Omega and Jalview. Supplementary Figure S1 is related to main Figure 1.

Supplementary Figure S2. *Xenopus* Brca2 protein (C-terminal half). (A) Alignment of *Xenopus* and Human Brca2 proteins including the region containing the helical domain, the oligonucleotide binding fold domains (OB1-3) and the Rad51-interacting domain (Rad51 ID) (highlighted). (B) Table showing identity and similarity of the different domains in human and *Xenopus* Brca2 proteins. Supplementary Figure S2 is related to main Figure 1.

Supplementary Figure S3. Anti Brca2 antibodies, Brca2 proteins and Brca2 chromatin binding. (A) Scheme showing the peptide region chosen to raise anti-*Xenopus* Brca2 antibodies. (B) WB of *Xenopus* egg extract (XE) in the presence of an excess of the Brca2 peptide used to generate Anti Brca2 antibodies or an excess of an unrelated control peptide (Un). (C) Chromatin binding time course in the presence of DMSO containing buffer or M-APH (20 μM). Chromatin was isolated at 60 and 90 min after addition of sperm nuclei and blotted with the indicated antibodies. (D) Chromatin binding time course of the indicated factors in the presence of chromosomal breakage. Chromatin was isolated at different times after addition of sperm nuclei and buffer or EcoRI (0.05 U/μl) restriction enzyme to egg extract and blotted with the indicated antibodies. (E) Chromatin binding of the indicated factors normalized to Histone H2B in Mock- and Brca2- depleted extracts. Mean optical density ± SD (n=3) is shown. (F) Scheme showing Brca2 domains included in Brca2c- and Brca2d-truncated proteins. (G) Coomassie-stained gels showing purification of GST-Brca2c and GST-Brca2d proteins before and

after PreScission mediated protease cleavage of the GST tag. Bands corresponding to Brca2c and Brca2d truncated proteins are indicated. Asterisks mark non-specific cleavage products. (H) Chromatin binding of the indicated proteins at 60 minutes from addition of sperm nuclei, S1 nuclease (0.1 U/μl) and L-APH (3 μM) in mock and Brca2 depleted extracts supplemented with 50 ng/μl Brca2c or Brca2d proteins. Supplementary Figure S3 is related to main Figure 1.

Supplementary Figure S4. DNA stability at replication forks and synthetic DNA overhangs. (A) Percentage of RIs with spontaneous fork gaps isolated from Mock-treated, Rad51-depleted or Brca2-depleted extracts supplemented with buffer or Mirin. Mean values ± SEM relative to 150 RIs counted in three experiments (n=3) are shown. (B) Percentage of RIs with H-APH-induced fork gaps isolated from extracts from Mock-treated or Brca2-depleted extracts supplemented with H-APH at 60 minutes from addition of sperm nuclei as shown in Figure 2E. Mean values ± SEM relative to 150 RIs counted in three experiments (n=3) are shown. (C) Fork gap size of RIs isolated from H-APH treated Mock- or Brca2-depleted extracts supplemented with buffer or Mirin. For each condition 100 RIs were scored. Median values with size range distribution are shown. (D) Percentage of single-stranded DNA replication bubbles isolated from Mock-treated or Brca2-depleted extracts supplemented with DMSO or H-APH at 60 minutes from addition of sperm nuclei as shown in Figure 2E. Mean values ± SEM relative to 90 RIs (n=3) are shown. (E) Relative percentage of residual biotin-dUTP in sperm nuclei quantified using a fluorescent method as in Figure 3A. Fluorescence intensity of Mock at 0 min was considered as 100%. Extracts were treated as indicated and supplemented with 100 μM Mirin or Buffer. Mean values ± SD in three experiments (n=3) are shown. (F) SDS-PAGE gel showing the indicated purified recombinant proteins. (G) Denaturing polyacrylamide gel showing the effect of the indicated amounts of Mre11 protein incubated with the fluorescently labeled synthetic 5' or 3' overhangs containing DNA substrates shown in the scheme. (H) Denaturing polyacrylamide gel showing $Rad51^{WT}$ and (I) RPA mediated protection from human Mre11 of fluorescently labeled 5'

overhang DNA substrate (20 nM) shown in Figure 3B. Increasing amounts of $Rad51^{WT}$ and RPA were used as indicated. Equivalent amounts of recombinant human Mre11 protein (hMre11, 30 nM) were added to the reactions as indicated. Supplementary Figure S4 is related to main Figures 2 and 3.

Supplementary Figure S5. Rad51-mediated protection of synthetic gapped DNA substrates. (A) Denaturing gels showing the effect of Rad51 WT, $Rad51^{T131P}$, or (B) RPA pre-incubation with the 5'-fluorescently labeled synthetic gapped DNA substrate (20 nM) containing phosphorothioate bonds (s) shown in the scheme and subsequent incubation with Mre11 protein (30 nM). (C) Mre11-dependent DNA degradation rates in the presence of $Rad51^{WT}$ or RPA relative to the amount of substrate (20 nM) shown in A, lane (-), which was considered as 100%. Mean values ± SEM (n=3) are shown. (D) DNA binding of $Rad51^{WT}$ or RPA to the fluorescently labeled synthetic gapped DNA substrate resolved on a 0.8% agarose gel. Supplementary Figure S5 is related to main Figure 3.

Supplementary Figure S6. Smarcal1 depletion-overexpression and RVF formation. (A) WB showing Smarcal1 in Mock and Smarcal1 depleted egg extract (lanes 1-2) and 1 and 5 ng of recombinant Smarcal1 protein (lanes 3-4). WB of egg extract using anti CDC45 and PCNA antibodies are also shown. (B) WB of Mock- and Smarcal1 depleted egg extracts using antibodies against the indicated factors. (C) Graph showing quantification of DNA replication for 120 minutes in Mock- and Smarcal1- depleted extracts as in Figure 1H. DNA replication in Mock was considered as 100%. Mean values ± SD in three experiments (n=3) are shown. (D) EM micrograph showing fork junction gap isolated from Smarcal1-depleted extract treated with H-APH as in Figure 2E. Empty arrows indicate replicated strands. Arrowhead indicates fork junction gap. (E) Graph showing fork junction gaps fold increase between Mock- and Smarcal1- depleted extracts treated with H-APH. Mean values ± SEM (n=3) are shown. (F) Graph showing EM quantification of RVFs following

increasing amounts of recombinant Smarcal1 protein added to extracts treated with H-APH added 45 min following nuclei addition to extracts. Reaction was allowed to proceed for additional 45 min. Graph shows a typical result. (G) EM micrograph showing replication bubble isolated from extracts treated with 25 ng/μl of Smarcal1. The inset shows magnification of the replication bubble with two reversed branches. (H) Chromatin binding time course of Flag-tagged recombinant Smarcal1^{WT} and Smarcal1^{HD} proteins added to egg extract (5 ng/μl) at the start of the reaction using anti Flag (Smarcal1) and anti MCM7 antibodies. Samples with buffer and no sperm addition (NS) are also shown. (I) ELISA detection of BrdU in nascent ssDNA as shown in Figure 4D in nuclei incubated in Mock- or Brca2 depleted extracts treated with Buffer or Mirin as indicated. Mean intensity values ± SD (n=3) are shown. Supplementary Figure S6 is related to main Figures 4 and 5.

Supplementary Figure S7. Function of Rad51 at replication forks. (A) Pol α NTD alignments from different species, with amino acids colored according to conservation and chemical nature. Possible structural elements present in the Pol α NTD are indicated below the alignment. (B) WB showing extract levels of Pol α and Rad51 after Mock treatment and Rad51 depletion. Relative intensity of Pol α (C), Pol δ (D) and Pol ε (E) nascent DNA binding in iPOND experiments normalized to Cdc45 in Mock-treated or Rad51-depleted extracts treated with buffer or M-APH (20 μM). Mean values ± SEM (n=3). (F) Scheme of restarting experiments. Sperm nuclei were added to Mock- or Rad51-depleted extracts, which were supplemented with M-APH according to scheme and incubated for additional 45 min (Stalling extract). Chromatin was then isolated and transferred to a second extract, which was depleted similar to stalling extracts and was supplemented with geminin and roscovitine (Restarting extract). DNA replication was monitored by incorporation of α-^{32}P-dCTP for 120 minutes. Supplementary Figure S7 is related to main Figure 6.